Arrangements

Nov 23 (Wed): No class, Thanksgiving!

Nov 28 (Mon): No class, time for you to work on Project 2

Dec 5 (Mon): Student Presentation 1

Dec 7 (Wed): Student Presentation 2

Deadlines:

Dec 5/Dec 7: Project 2 Presentation File due at 12noon

Dec 9 (Fri): Project 2 Summary of Another Team's Work due at 11:59pm

Dec 12 (Mon): Project 2 Final Report due at 11:59pm

Summary

- Topics:

1. Bio-medical imaging
2. Image processing
3. Geometric modeling and computer graphics
4. Mesh generation
   - Marching Cubes/Dual Contouring
   - Tri/Tet Meshing
   - Quad/Hex Meshing
   - Quality Improvement
5. Computational mechanics
6. Bio-medical applications

Topic 5: Extended Finite Element Method (X-FEM) and Immersed Finite Element Method (IFEM)

Jessica Zhang
Department of Mechanical Engineering
Courtesy Appointment in Biomedical Engineering
Carnegie Mellon University
jessicaz@andrew.cmu.edu
http://www.andrew.cmu.edu/user/jessicaz

Extended Finite Element Method (X-FEM)

Extended Finite Element Method (X-FEM)

• The initial developments of the X-FEM took place at Northwestern University (T. Belytschko 2000).

FEM

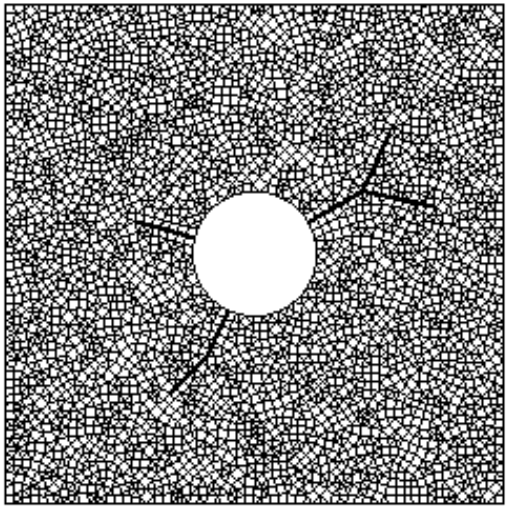

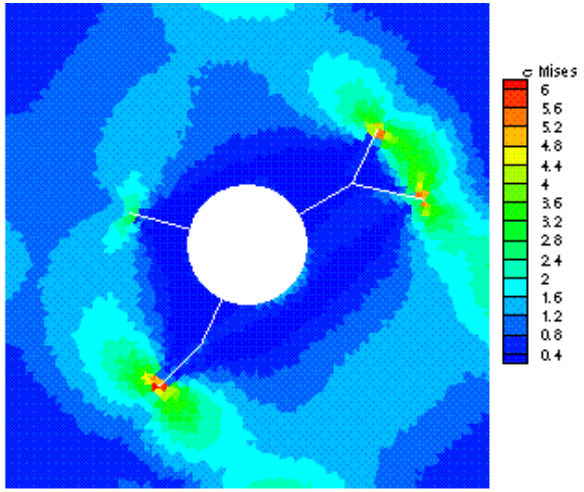

X-FEM

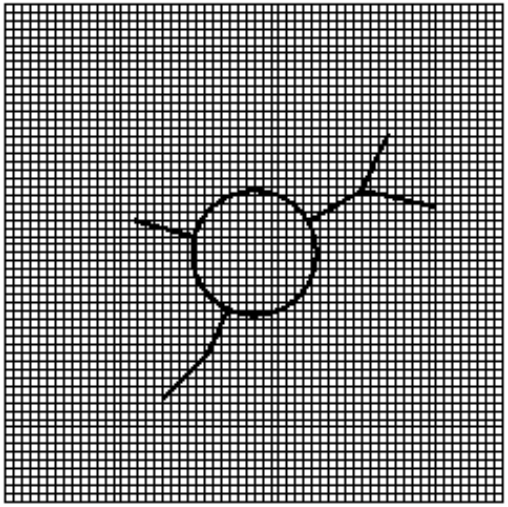

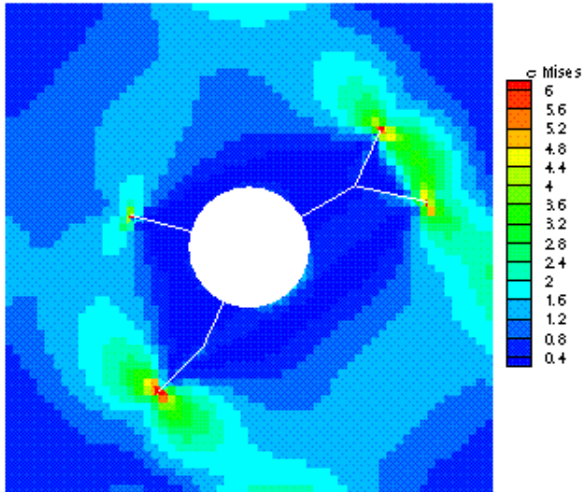

Extended Finite Element Method (X-FEM)

- In the X-FEM, a standard displacement based finite element approximation is enriched by additional (special) functions using the framework of partition of unity. It is a particular instance of the partition of unity finite element method (PUFEM) or the generalized finite element method (GFEM).

- In the X-FEM, the finite element mesh need not conform to the internal boundaries (cracks, material interfaces, voids, etc.), and hence a single mesh suffices for modeling as well as capturing the evolution of material interfaces and cracks in two- and three-dimensions.

Background

- Solving crack problems in fracture mechanics is imperative to quantify and predict the behavior of cracked structures under service conditions.

- To this end, the accurate evaluation of fracture parameters such as the stress intensity factors (SIF) is required for simulation-based life-cycle design analysis.

Background

- Over the past few decades, many numerical methods have been proposed to model crack problems. Finite element methods with non-singular and singular elements enable the accurate computation of stress intensity factors. However, these methods require the finite element edges to coincide with the crack. This often complicates mesh generation, since both the regular geometric features and the crack must be considered.

- Some of the other prominent numerical methods for crack analysis are the boundary elements method, the boundary collocation method, the body force method and the integral equation method. The dislocation method is also often used for cracks with multiple branches. Recently, meshless methods, and in particular the element-free Galerkin method, have been applied to two-dimensional crack problems.

X-FEM

- The extended finite element method (X-FEM) allows for the modeling of arbitrary geometric features independently of the finite element mesh.

- This method allows the modeling of crack growth without remeshing. This facilitates the accurate modeling of interactions between cracks and holes, or systems with cracks emanating from holes.

- The partition of unity is used as a means to enrich a finite element space.

Governing Equations for Elastostatics

Consider the domain Ω bounded by Γ. The boundary Γ is composed of Γ_u, Γ_t, Γ_c and Γ_h such that $\Gamma = \Gamma_u \cup \Gamma_t \cup \Gamma_c \cup \Gamma_h$ as shown in Figure 1. Prescribed displacements are imposed on Γ_u, while prescribed tractions are imposed on Γ_t. The boundary Γ_c consists of the boundaries of all cracks (both faces for each crack) and Γ_h gathers all boundaries of holes. The hole and crack faces are assumed to be traction-free. The equilibrium equations and the boundary conditions are

$$\begin{aligned} \nabla \cdot \boldsymbol{\sigma} + \mathbf{b} &= 0 \text{ in } \Omega \\ \mathbf{u} &= \bar{\mathbf{u}} \text{ on } \Gamma_u \\ \boldsymbol{\sigma} \cdot \mathbf{n} &= \bar{\mathbf{t}} \text{ on } \Gamma_t \\ \boldsymbol{\sigma} \cdot \mathbf{n} &= 0 \text{ on } \Gamma_c \\ \boldsymbol{\sigma} \cdot \mathbf{n} &= 0 \text{ on } \Gamma_h \end{aligned}$$

where $\mathbf{n}$ is the unit outward normal, $\boldsymbol{\sigma}$ the Cauchy stress, and $\mathbf{b}$ is the body force per unit volume.

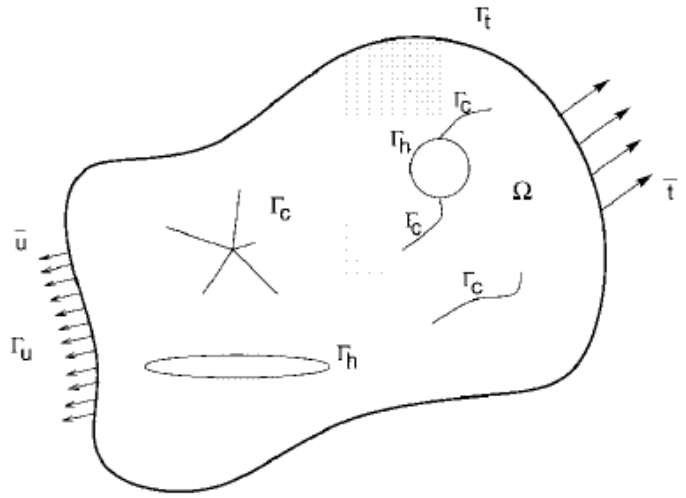

Governing Equations for Elastostatics

We consider small strains and displacements. The kinematics equations therefore consist of the strain-displacement relation

$$\boldsymbol{\varepsilon} = \boldsymbol{\varepsilon}(\mathbf{u}) = \nabla_s \mathbf{u}$$

where ∇_s is the symmetric part of the gradient operator. The constitutive relation is given by Hooke's law

$$\boldsymbol{\sigma} = \mathbf{C}\boldsymbol{\varepsilon}$$

where $\mathbf{C}$ is Hooke's tensor.

Weak Form

- The space of trial functions is defined by

$$\mathscr{U} = \{\mathbf{u} \in \mathscr{V} : \mathbf{u} = \bar{\mathbf{u}} \text{ on } \Gamma_u, \ \mathbf{u} \text{ discontinuous on } \Gamma_c \cup \Gamma_h\}$$

  where the space V is related to the regularity of the solution.

- The test function space is defined similarly as

$$\mathscr{U}_0 = \{\mathbf{v} \in \mathscr{V} : \mathbf{v} = 0 \text{ on } \Gamma_u, \ \mathbf{v} \text{ discontinuous on } \Gamma_c \cup \Gamma_h\}$$

- The weak form of the equilibrium equations is given by

$$\int_\Omega \boldsymbol{\sigma}(\mathbf{u}) : \boldsymbol{\varepsilon}(\mathbf{v}) \ d\Omega = \int_\Omega \mathbf{b} \cdot \mathbf{v} \ d\Omega + \int_{\Gamma_t} \bar{\mathbf{t}} \cdot \mathbf{v} \ d\Gamma \quad \forall \mathbf{v} \in \mathscr{U}_0$$

- Using the constitutive relation and the strain-displacement relation, the weak form can be stated as: find $\mathbf{u} \in \mathscr{U}$ such that

$$\int_\Omega \boldsymbol{\varepsilon}(\mathbf{u}) : \mathbf{C} : \boldsymbol{\varepsilon}(\mathbf{v}) \ d\Omega = \int_\Omega \mathbf{b} \cdot \mathbf{v} \ d\Omega + \int_{\Gamma_t} \bar{\mathbf{t}} \cdot \mathbf{v} \ d\Gamma \quad \forall \mathbf{v} \in \mathscr{U}_0$$

Modeling a Branched Crack with the X-FEM

- A crack can be modeled independently of the mesh by enriching the approximation by step functions and asymptotic near-tip fields. The finite element approximation for a single crack in a two-dimensional body can be written as

$$\mathbf{u}^h(\mathbf{x}) = \sum_{i\in I} \mathbf{u}_i \phi_i(\mathbf{x}) + \sum_{i\in L} \mathbf{a}_i \phi_i(\mathbf{x}) H(\mathbf{x}) + \sum_{i\in K_1} \phi_i(\mathbf{x}) \left(\sum_{l=1}^{4} \mathbf{b}_{i,1}^l F_1^l(\mathbf{x}) \right) + \sum_{i\in K_2} \phi_i(\mathbf{x}) \left(\sum_{l=1}^{4} \mathbf{b}_{i,2}^l F_2^l(\mathbf{x}) \right)$$

where I is the set of all nodes in the mesh; $\mathbf{u}_i$ is the classical (vectorial) degree of freedom at node i; ϕ_i is the shape function associated with node i. Each shape function ϕ_i has compact support ω_i given by the union of the elements connected to node i; $L \subset I$ is the subset of nodes that are enriched for the crack discontinuity and $\mathbf{a}_i$ are the corresponding additional degrees of freedom; the nodes in L are such that their support (we mean the support of the nodal shape function) intersects the crack but do not contain any of its crack tips; and $K_1 \subset I$ and $K_2 \subset I$ are the subset of nodes that are enriched for the first and second crack tip, respectively. The corresponding additional degrees of freedom are $\mathbf{b}_{i,1}^l$ and $\mathbf{b}_{i,2}^l$, $l = 1,\ldots,4$, for the first and second crack tip, respectively; the nodes in K_1 (K_2) are such that their support contain the first (second) crack tip.

Modeling a Branched Crack with the X-FEM

The near-tip functions $F_1^l(\mathbf{x})$, $l = 1, \ldots, 4$, are given by

$$\{F_1^l(\mathbf{x})\} \equiv \left\{ \sqrt{r}\sin\left(\frac{\theta}{2}\right), \sqrt{r}\cos\left(\frac{\theta}{2}\right), \sqrt{r}\sin\left(\frac{\theta}{2}\right)\sin(\theta), \sqrt{r}\cos\left(\frac{\theta}{2}\right)\sin(\theta) \right\}$$

where (r, θ) are the local polar coordinates at the first crack tip with θ=0 coinciding with the tangent to the crack at the tip. Similarly, the near-tip functions $F_2^l(\mathrm{x})$ are also given by the above equation but the local polar co-ordinates being now defined at the second crack tip.

The function $H(\mathrm{x})$ is a discontinuous function across the crack surface and is constant on each side of the crack: +1 on one side of the crack and −1 on the other. The crack is considered to be a curve parameterized by the curvilinear coordinate s.

A smooth crack

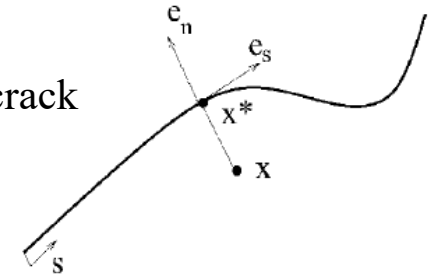

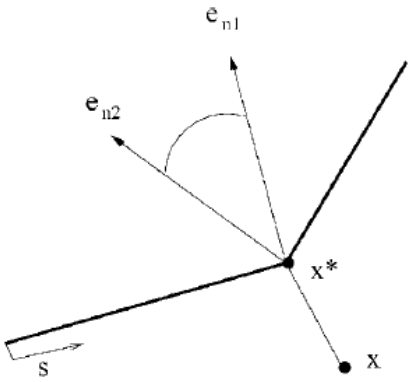

A kinked crack

Branched Cracks

- We first consider a simple case of a branched crack modeled by four elements. We wish to illustrate how an equivalent discrete space can be constructed with the X-FEM mesh by enriching with the discontinuous function $H(x)$ and another function which takes into account the junction between the three branches.

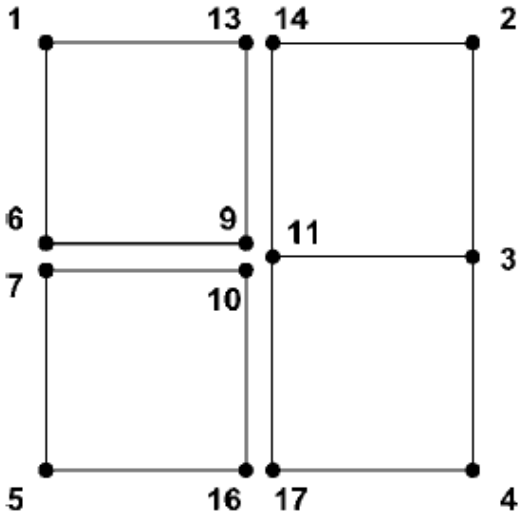

FEM mesh

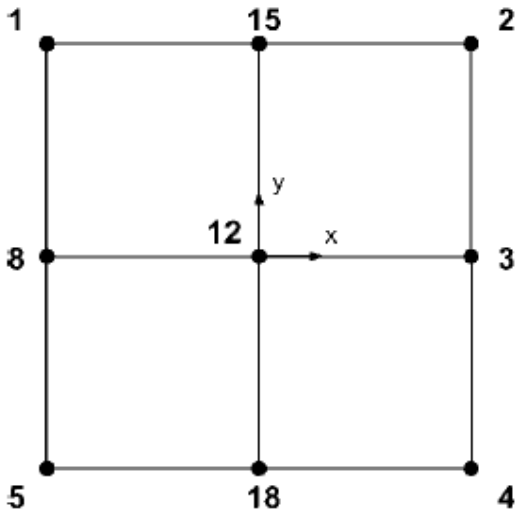

X-FEM mesh

Branched Cracks

- The finite element approximation associated with the FE mesh is

$$\mathbf{u}^h(\mathbf{x}) = \sum_{i \in I} \mathbf{u}_i \phi_i(\mathbf{x}), \quad I = \{1, \ldots, 17\}$$

where u_i is the displacement at node i and ϕ_i is the bilinear shape function associated with node i. Let us introduce the nodal vectorial variables α_8, β_8, α_{15}, β_{15}, α_{18}, β_{18}, α_{12}, β_{12} and γ_{12} such that

$$\alpha_8 = \frac{\mathbf{u}_6 + \mathbf{u}_7}{2}, \qquad \beta_8 = \frac{\mathbf{u}_6 - \mathbf{u}_7}{2}$$

$$\alpha_{15} = \frac{\mathbf{u}_{13} + \mathbf{u}_{14}}{2}, \qquad \beta_{15} = \frac{\mathbf{u}_{14} - \mathbf{u}_{13}}{2}$$

$$\alpha_{18} = \frac{\mathbf{u}_{16} + \mathbf{u}_{17}}{2}, \qquad \beta_{18} = \frac{\mathbf{u}_{17} - \mathbf{u}_{16}}{2}$$

$$\alpha_{12} = \frac{\mathbf{u}_{11} + (\mathbf{u}_9 + \mathbf{u}_{10})/2}{2}, \qquad \gamma_{12} = \frac{\mathbf{u}_9 - \mathbf{u}_{10}}{2}$$

$$\beta_{12} = \frac{\mathbf{u}_{11} - (\mathbf{u}_9 + \mathbf{u}_{10})/2}{2},$$

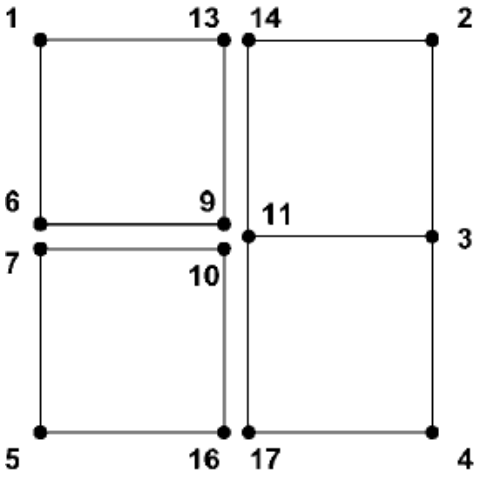

FEM mesh

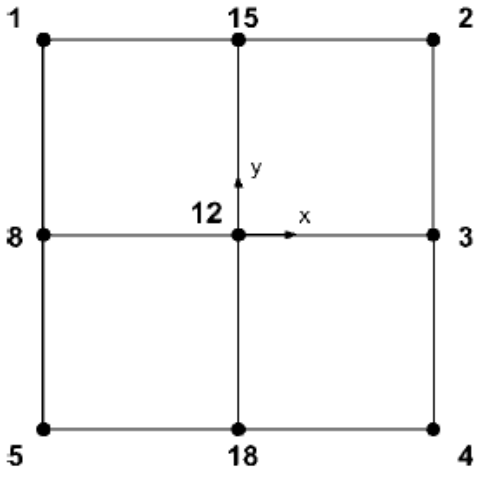

X-FEM mesh

Branched Cracks

- Inverting the previous system, we obtain the following equations:

$$\mathbf{u}_6 = \alpha_8 + \beta_8, \qquad \mathbf{u}_7 = \alpha_8 - \beta_8$$
$$\mathbf{u}_9 = \alpha_{12} - \beta_{12} + \gamma_{12}, \qquad \mathbf{u}_{10} = \alpha_{12} - \beta_{12} - \gamma_{12}$$
$$\mathbf{u}_{11} = \alpha_{12} + \beta_{12}, \qquad \mathbf{u}_{13} = \alpha_{15} - \beta_{15}$$
$$\mathbf{u}_{14} = \alpha_{15} + \beta_{15}, \qquad \mathbf{u}_{16} = \alpha_{18} - \beta_{18}$$
$$\mathbf{u}_{17} = \alpha_{18} + \beta_{18}$$

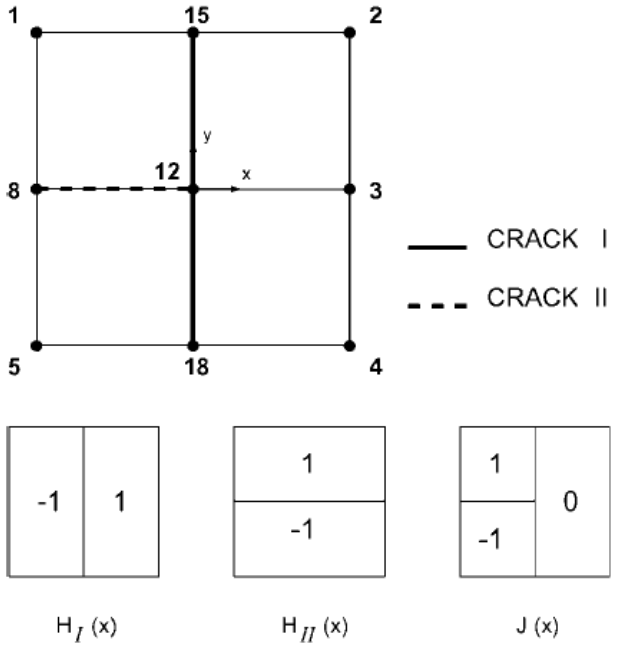

- We have

$$\mathbf{u}^h = \sum_{i=1}^{5} \mathbf{u}_i \phi_i + \alpha_8(\phi_6 + \phi_7) + \beta_8 H_{\mathrm{II}}(\mathbf{x})(\phi_6 + \phi_7)$$
$$+ \alpha_{12}(\phi_9 + \phi_{10} + \phi_{11}) + \beta_{12} H_{\mathrm{I}}(\mathbf{x})(\phi_9 + \phi_{10} + \phi_{11})$$
$$+ \gamma_{12} J(\mathbf{x})(\phi_9 + \phi_{10})$$
$$+ \alpha_{15}(\phi_{13} + \phi_{14}) + \beta_{15} H_{\mathrm{I}}(\mathbf{x})(\phi_{13} + \phi_{14})$$
$$+ \alpha_{18}(\phi_{16} + \phi_{17}) + \beta_{18} H_{\mathrm{I}}(\mathbf{x})(\phi_{16} + \phi_{17})$$

Branched Cracks

- We next relate the functions $H_I(x)$ and $H_{II}(x)$ to the function $H(x)$. Deciding that crack I is parameterized so that we traverse it from nodes 15 to 18 and that crack II is parameterized so that we traverse it from nodes 8 to 12, the functions $H_I(x)$ and $H_{II}(x)$ are then the function $H(x)$ associated with cracks I and II, respectively.
- The function $J(x)$ is referred to as a discontinuous "junction" function. It may be expressed in terms of the functions $H_I(x)$ and $H_{II}(x)$ as

$$J(\mathbf{x}) = \begin{cases} H_{II}(\mathbf{x}) & \text{for } H_I(\mathbf{x}) < 0 \\ 0 & \text{for } H_I(\mathbf{x}) > 0 \end{cases}$$

Branched Cracks

- If we now consider the X-FEM mesh, $\phi_6 + \phi_7$, $\phi_9 + \phi_{10} + \phi_{11}$, $\phi_{13} + \phi_{14}$, $\phi_{16} + \phi_{17}$ can be replaced by ϕ_8, ϕ_{12}, ϕ_{15}, ϕ_{18}, respectively, and α_8, α_{12}, α_{15}, α_{18} by $\mathbf{u}_8$, $\mathbf{u}_{12}$, $\mathbf{u}_{15}$, $\mathbf{u}_{18}$. The finite element approximation now reads

$$\begin{aligned}\mathbf{u}^h = & \sum_{i \in I'} \mathbf{u}_i \phi_i \\ & + \boldsymbol{\beta}_{12}\phi_{12}H_{\mathrm{I}}(\mathbf{x}) + \boldsymbol{\beta}_{15}\phi_{15}H_{\mathrm{I}}(\mathbf{x}) + \boldsymbol{\beta}_{18}\phi_{18}H_{\mathrm{I}}(\mathbf{x}) \\ & + \boldsymbol{\beta}_{8}\phi_{8}H_{\mathrm{II}}(\mathbf{x}) \\ & + \boldsymbol{\gamma}_{12}\phi_{12}J(\mathbf{x})\end{aligned}$$

where I' = {1, 2, 3, 4, 5, 8, 12, 15, 18}. The first term on the right-hand side represents the classical finite element approximation associated with the mesh and the next four represent the discontinuous enrichment for cracks I and II taken separately, finally, the last term takes into account the junction. This shows that the discrete spaces obtained by FEM and X-FEM are equivalent for a branched crack aligned with the mesh.

Branched Cracks

- We now extend the derivation to the case where the branched crack geometry is represented independently of the mesh. Consider the below branched crack. Let us view this crack as a main crack (solid line) and a branched secondary crack (dashed line).
- The enrichment proceeds as follows. The main crack is enriched as if the secondary crack were absent. This enrichment involves the tip enrichments for the crack tips B and C. The secondary crack is enriched almost as if the main crack was absent: the tip D is enriched (plus) and all nodes for which the support intersects the secondary crack but do not contain points A or D are part of the discontinuous interior enrichment (diamonds). Finally, we need to enrich for the junction: the junction function is added to all nodes for which the support of the finite element shape functions contain the junction point A (crosses).

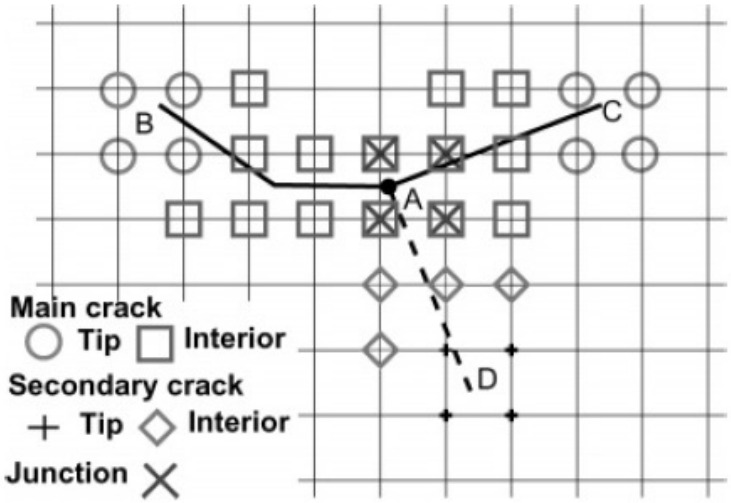

Cracks with Multiple Branches

- Having introduced the junction function $J(x)$, we now describe how we can extend it to model multiple branched cracks. In the case of crossing cracks, the first idea that comes to mind is to consider the two cracks as independent cracks. But it is easy to show that this approach is incorrect.
- In essence, using the X-FEM, we recast the independent unknowns in the FEM discretization in a different form. For multiple branched crack, we must have the same number of degrees of freedom per node as twice (n_D =2) the number of pieces its support are cut into. Thus, the procedure for modeling a multiple branched crack consists of discretizing the branched crack into a main crack and several cracks joining the main crack. This approach leads to the right number of degrees of freedom per node.

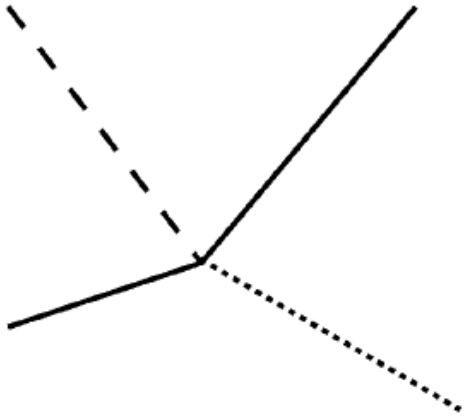

Figure 8. A crack with multiple branches, ——= main crack, - - - = secondary 1, – – – = secondary 2.

Cracks with Multiple Branches

- Consider now a main crack to which several secondary cracks are connected. We assume that the main and the secondary cracks do not have any branches, although it is easy to generalize to this case. Let N_c be the number of cracks (the main crack plus the number of secondary cracks), N_t be the number of crack tips and N_x be the number of junctions ($N_x = N_c - 1$). The displacement approximation is

$$\mathbf{u}^h(\mathbf{x}) = \sum_{i\in I} \mathbf{u}_i \phi_i(\mathbf{x}) + \sum_{j=1}^{N_c} \sum_{i\in L_j} \mathbf{a}_{i,j} \phi_i(\mathbf{x}) H_j(\mathbf{x}) + \sum_{j=1}^{N_t} \sum_{i\in K_j} \phi_i(\mathbf{x}) \left(\sum_{l=1}^{4} \mathbf{b}_{i,j}^l F_j^l(\mathbf{x}) \right) + \sum_{j=1}^{N_x} \sum_{i\in J_j} \mathbf{c}_{i,j} \phi_i(\mathbf{x}) J_j(\mathbf{x})$$

(1) $L_j \subset I$ is the subset of nodes to enrich for the jth crack discontinuity and $\mathbf{a}_{i,j}$ are the corresponding additional degrees of freedom; the nodes in L_j are such that their support intersects the jth crack but do not contain any of its two extremities;

(2) $K_j \subset I$ is the subset of nodes to enrich for the jth crack tip and $\mathbf{b}_{i,j}^l$, $l = 1, \ldots, 4$, are the corresponding additional degrees of freedom; the nodes in K_j are such that their support contain the jth crack tip;

(3) $J_j \subset I$ is the subset of nodes to enrich for the jth junction and $\mathbf{c}_{i,j}$ are the corresponding additional degrees of freedom; the nodes in J_j are such that their support contain the jth junction.

Modeling Holes with the X-FEM

- We show here how to model holes which are not defined by the mesh. The idea is to define an enrichment function $V(\mathrm{x})$ which is zero in the holes and one in the body

$$V(\mathbf{x}) = \begin{cases} 1 & \text{if } \mathbf{x} \in \Omega \\ 0 & \text{if } \mathbf{x} \notin \Omega \end{cases}$$

where Ω is the domain occupied by the body. If the support of a nodal shape function intersects a hole, the nodal shape function is multiplied by the $V(\mathrm{x})$ function so that the support size is reduced to its material fraction. Also, the nodal degrees of freedom for which the support are totally in the void are eliminated (or set to zero depending on the implementation).

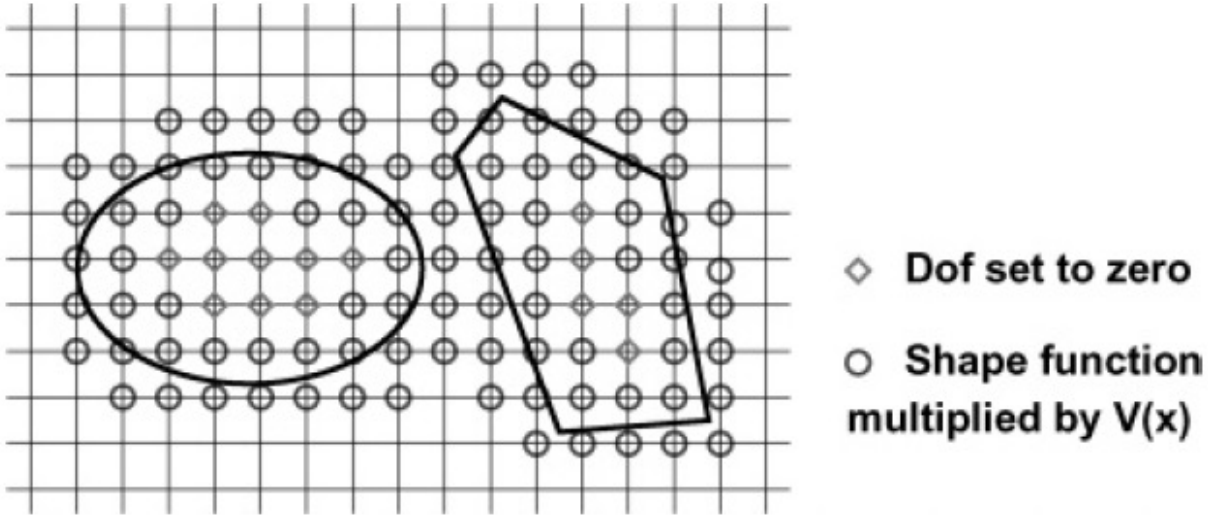

Modeling Holes with the X-FEM

- To model a crack emanating from a hole, we only have to replace the classical shape functions $\phi_i(\mathbf{x})$ by $\psi_i(\mathbf{x}) = V(\mathbf{x})\phi_i(\mathbf{x})$ and to set to zero all the degrees of freedom attached to a node whose support is entirely in the hole.
- In practice, we do not replace the classical shape functions $\phi_i(\mathbf{x})$ by $\psi_i(\mathbf{x}) = V(\mathbf{x})\phi_i(\mathbf{x})$, we simply omit the integral in the holes. Furthermore, we replace the area A_ω by $A_\omega - A_{\text{hole}}$, where A_{hole} is the area of the nodal support in the hole.
- Note that since the function is discontinuous on the boundary of the holes, zero tractions are automatically implied by the weak form.

Summary of X-FEM

- The X-FEM has been developed for modeling arbitrary geometries such as multiple branched cracks, voids and cracks emanating from holes without the need for the geometric entities to be meshed. The classical FEM approximation is enriched by the asymptotic near-tip field, the discontinuous function and a new discontinuous function to account for the multiple branched crack.

- The voids are modeled by applying a quadrature scheme which partitions elements along the boundary of the voids and only considers the integrals within the body.

- The relative ease of crack growth simulation without remeshing and the treatment of various flaws within a unified framework are, however, overriding advantages of the X-FEM over existing FE-based technology for modeling cracks.

Summary of X-FEM

- The striking advantages are that the finite element framework (sparsity and symmetry of the stiffness matrix) is retained, and a single-field variational principle is used.

- Related links

  A touch of nostalgia on the NWU-connection:

  http://dilbert.engr.ucdavis.edu/~suku/xfem/nostalgia.html

Immersed Finite Element Method (IFEM)

Immersed Boundary Element Method

- In the 1970s, Peskin developed the immersed boundary (IB) method to study flow patterns around heart valves. The mathematical formulation of the IB method employs a mixture of Eulerian and Lagrangian descriptions for fluid and solid domains.
- In particular, the entire fluid domain is represented by a uniform background grid, which can be solved by finite difference methods with periodic boundary conditions, whereas the submerged structure is represented by a fiber network.
- The interaction between fluid and structure is accomplished by distributing the nodal forces and interpolating the velocities between the Eulerian and Lagrangian domains through a smoothed approximation of the Dirac delta function.
- The advantage of the IB method is that the fluid-structure interface is tracked automatically, which circumvents one of the most costly computations, namely mesh update algorithms.

http://www.math.nyu.edu/faculty/peskin/

Drawbacks of Immersed BM

- Nevertheless, one major disadvantage of the IB method is the assumption of a fiber-like one-dimensional immersed structure, which may carry mass, but occupies no volume in the fluid domain.
- This assumption also limits accurate representation of immersed flexible solids which may occupy finite volumes within the fluid domain.
- Furthermore, uniform fluid grids also set limitations in resolving fluid domains with complex shapes and boundary conditions.

Immersed FEM

- Following the pioneering work of Peskin and co-workers on the IB method, an alternative approach, the immersed finite element method (IFEM) was developed.

- This method is able to eliminate the aforementioned drawbacks of the IB method. With finite element formulations for both fluid and solid domains, the submerged structure is solved more realistically and accurately in comparison with the corresponding fiber network representation.

IFEM

- Let us consider an incompressible 3D deformable structure in Ω^s completely immersed in an incompressible fluid domain Ω^f. Together, the fluid and the solid occupy a domain Ω, but they do not intersect:

$$\Omega^f \cup \Omega^s = \Omega,$$

$$\Omega^f \cap \Omega^s = \emptyset.$$

- In contrast to the IB formulation, the solid domain can occupy a finite volume in the fluid domain. Since we assume both fluid and solid to be incompressible, the union of two domains can be treated as one incompressible continuum with a continuous velocity field.
- In the computation, the fluid spans the entire domain Ω, thus an Eulerian fluid mesh is adopted, whereas a Lagrangian solid mesh is constructed on top of the Eulerian fluid mesh.
- The coexistence of fluid and solid in Ω^s requires some considerations when developing the momentum and continuity equations.

IFEM

- In the computational fluid domain Ω, the fluid grid is represented by the time-invariant position vector x; while the material points of the structure in the initial solid domain Ω_0^s and the current solid domain Ω^s are represented by X^s and $x^s(X^s, t)$, respectively.
- In the fluid calculations, the velocity v and the pressure p are the unknown fluid field variables; whereas the solid domain involves the calculation of the nodal displacement u^s, which is defined as the difference of the current and the initial coordinates: $u^s = x^s - X^s$. The velocity v^s is the material derivative of the displacement du^s/dt.

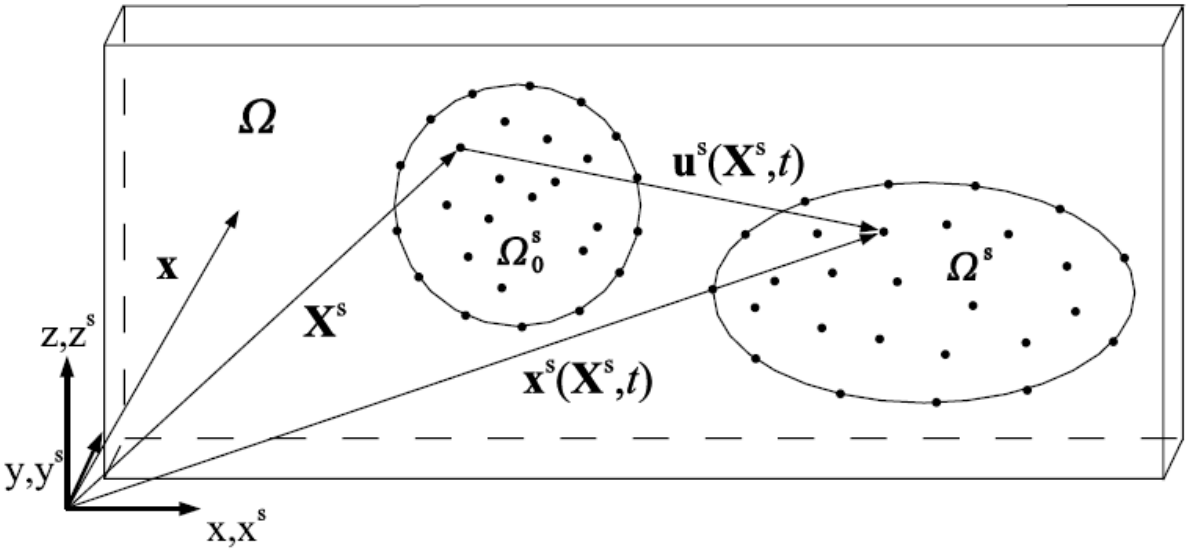

IFEM

- We define the fluid-structure interaction force within the domain Ω^{s} as $f_i^{\mathrm{FSI,s}}$,

$$f_i^{\mathrm{FSI,s}} = -(\rho^{\mathrm{s}} - \rho^{\mathrm{f}})\frac{\mathrm{d}v_i}{\mathrm{d}t} + \sigma_{ij,j}^{\mathrm{s}} - \sigma_{ij,j}^{\mathrm{f}} + (\rho^{\mathrm{s}} - \rho^{\mathrm{f}})g_i, \quad \mathbf{x} \in \Omega^{\mathrm{s}}.$$

- A Dirac delta function δ is used to distribute the interaction force from the solid domain onto the computational fluid domain:

$$f_i^{\mathrm{FSI}}(\mathbf{x}, t) = \int_{\Omega^{\mathrm{s}}} f_i^{\mathrm{FSI,s}}(\mathbf{x}^{\mathrm{s}}, t)\,\delta(\mathbf{x} - \mathbf{x}^{\mathrm{s}}(\mathbf{X}^{\mathrm{s}}, t))\,\mathrm{d}\Omega.$$

IFEM

- The governing equation for the fluid can be derived by combining the fluid terms and the interaction force as

$$\rho^{\mathrm{f}} \frac{\mathrm{d}v_i}{\mathrm{d}t} = \sigma^{\mathrm{f}}_{ij,j} + f_i^{\mathrm{FSI}}, \quad \mathbf{x} \in \Omega.$$

- The entire domain is incompressible: $v_{i,i} = 0$.

- To delineate the Lagrangian description for the solid and the Eulerian description for the fluid, we introduce different velocity field variables v_i^{s} and v_i to represent the motions of the solid in the domain Ω^{s} and the fluid within the entire domain Ω. The coupling of both velocity fields is accomplished with the Dirac delta function:

$$v_i^{\mathrm{s}}(\mathbf{X}^{\mathrm{s}}, t) = \int_{\Omega} v_i(\mathbf{x}, t)\delta(\mathbf{x} - \mathbf{x}^{\mathrm{s}}(\mathbf{X}^{\mathrm{s}}, t))\,\mathrm{d}\Omega.$$

IFEM

- Let us assume that there is no traction applied on the fluid boundary, i.e. $\int_{\Gamma_{h_i}} \delta v_i h_i \, \mathrm{d}\Gamma = 0$, applying integration by parts and the divergence theorem, we can get the final weak form (with stabilization terms):

$$\int_\Omega \left(\delta v_i + \tau^m v_k \, \delta v_{i,k} + \tau^c \, \delta p_{,i}\right)\left[\rho^f (v_{i,t} + v_j v_{i,j}) - f_i^{FSI}\right] \mathrm{d}\Omega + \int_\Omega \delta v_{i,j} \sigma_{ij}^f \, \mathrm{d}\Omega$$
$$- \sum_e \int_{\Omega_e} \left(\tau^m v_k \, \delta v_{i,k} + \tau^c \, \delta p_{,i}\right) \sigma_{ij,j}^f \, \mathrm{d}\Omega + \int_\Omega (\delta p + \tau^c \, \delta v_{i,i}) v_{j,j} \, \mathrm{d}\Omega = 0.$$

  where τ^m and τ^c are the scalar stabilization parameters dependent of the computational grid, time step size, and flow variables.
- The non-linear systems are solved with the Newton-Raphson method.

IFEM

- The transformation of the weak form from the updated Lagrangian to the total Lagrangian description is to change the integration domain from Ω^{s} to Ω_0^{s}. Since we consider an incompressible fluid and solid, and the Jacobian determinant is 1 in the solid domain, the transformation of the weak form to total Lagrangian description yields

$$\int_{\Omega_0^{\mathrm{s}}} \delta u_i \left[(\rho^{\mathrm{s}} - \rho^{\mathrm{f}}) \ddot{u}_i^{\mathrm{s}} - \frac{\partial P_{ji}}{\partial X_j^{\mathrm{s}}} - (\rho^{\mathrm{s}} - \rho^{\mathrm{f}}) g_i + f_i^{\mathrm{FSI,s}} \right] \mathrm{d}\Omega_0^{\mathrm{s}} = 0,$$

  where the first Piola-Kirchhoff stress P_{ij} is defined as $P_{ij} = JF_{ik}^{-1}\sigma_{kj}^{\mathrm{s}}$ and the deformation $F_{ij} = \partial x_i^{\mathrm{s}} / \partial X_j^{\mathrm{s}}$.

- Using integration by parts and the divergence theorem, we can obtain

$$\int_{\Omega_0^{\mathrm{s}}} \delta u_i (\rho^{\mathrm{s}} - \rho^{\mathrm{f}}) \ddot{u}_i^{\mathrm{s}} \, \mathrm{d}\Omega_0^{\mathrm{s}} + \int_{\Omega_0^{\mathrm{s}}} \delta u_{i,j} P_{ji} \, \mathrm{d}\Omega_0^{\mathrm{s}} - \int_{\Omega_0^{\mathrm{s}}} \delta u_i (\rho^{\mathrm{s}} - \rho^{\mathrm{f}}) g_i \, \mathrm{d}\Omega_0^{\mathrm{s}} + \int_{\Omega_0^{\mathrm{s}}} \delta u_i f_i^{\mathrm{FSI,s}} \, \mathrm{d}\Omega_0^{\mathrm{s}} = 0.$$

IFEM

- For structures with large displacements and deformations, the second Piola-Kirchhoff stress S_{ij} and the Green-Lagrangian strain E_{ij} are used in the total Lagrangian formulation:

$$S_{ij} = \frac{\partial W}{\partial E_{ij}} \quad \text{and} \quad E_{ij} = \frac{1}{2}(C_{ij} - \delta_{ij}),$$

  where W is the elastic energy potential and C is the Green-Lagrangian deformation tensor. The first Piola-Kirchhoff stress P_{ij} can be obtained from the second Piola-Kirchhoff $P_{ij} = S_{ik}F_{jk}$.
- Finally, in the interpolation process from the fluid onto the solid grid,

$$v_{iI}^{s} = \sum_{J} v_{iJ}(t)\phi_J(\mathbf{x}_J - \mathbf{x}_I^{s}), \quad \mathbf{x}_J \in \Omega_{\phi I}.$$

  A dual procedure takes place in the distribution process from the solid onto the fluid grid,

$$f_{iJ}^{\mathrm{FSI}} = \sum_{I} f_{iI}^{\mathrm{FSI,s}}(\mathbf{X}^{s}, t)\phi_I(\mathbf{x}_J - \mathbf{x}_I^{s}), \quad \mathbf{x}_I^{s} \in \Omega_{\phi J}.$$

- By interpolating the fluid velocities onto the solid particles, the fluid within the solid domain is bounded to solid material points. This ensures not only the no-slip boundary condition on the surface of the solid, but also automatically stops the fluid from penetrating the solid.

Application to Biological Systems

- There are various scales involved in a biological system such as the multiple scale phenomena in the cardiovascular system. The objective is to predict blood flow, its effect on the blood vessels and in turn the effect on the blood cells, which are interrelated.

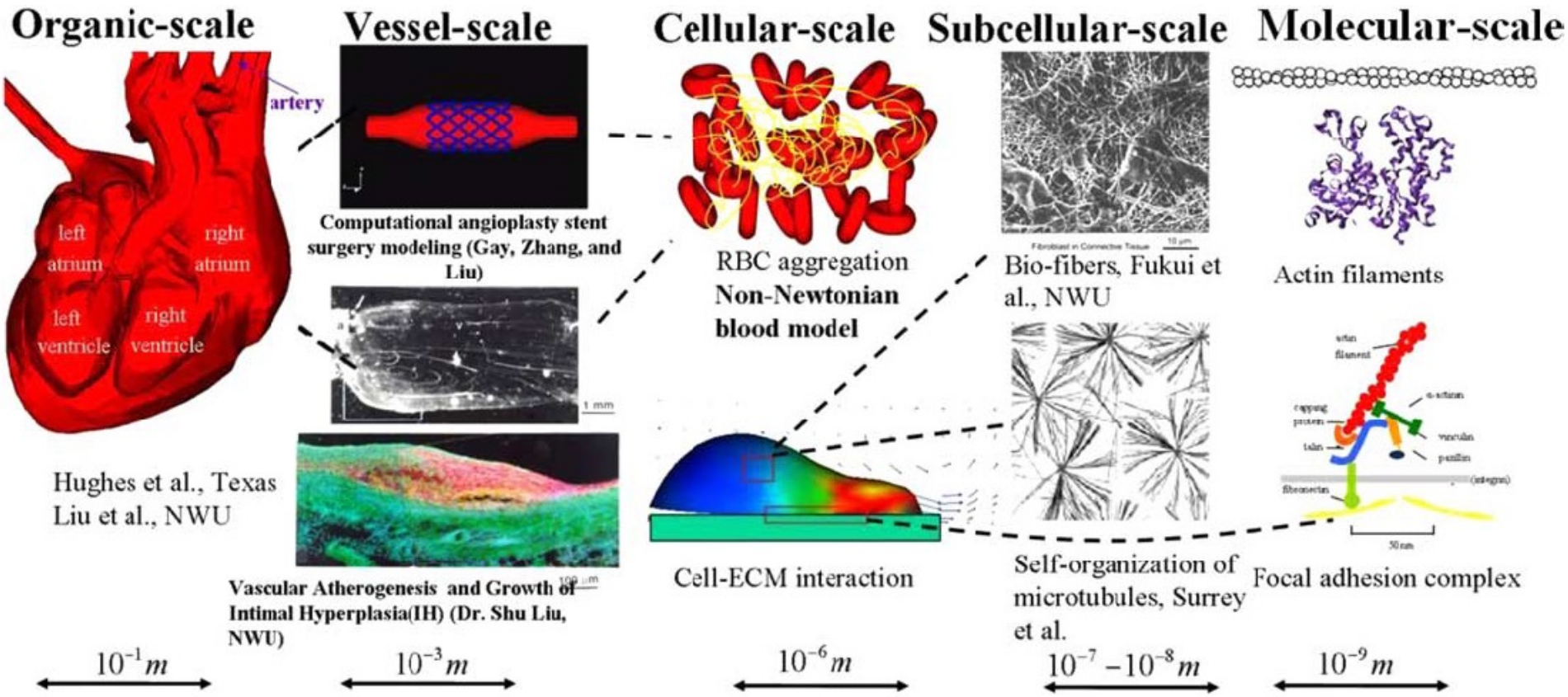

Summary of IFEM

- IFEM chooses finite element formulations for both fluid and solid domains.
- The fluid solver is based on a stabilized equal-order finite element formulation applicable to problems involving moving boundaries. This stabilized formulation prevents numerical oscillations without introducing excessive numerical dissipation.
- Moreover, in the IFEM, the background fluid mesh does not have to follow the motion of the flexible fluid-structure interfaces and thus it is possible to assign a sufficiently refined fluid mesh within the region around the immersed, moving, deformable structures.

Immersed FEM

- Unlike the Dirac delta functions in the IB method which yield C^1 continuity, the discretized delta function in IFEM is the C^n shape function often employed in the meshfree reproducing Kernel particle method (RKPM).
- Because of the higher order smoothness in the RKPM delta function, the accuracy is increased in the coupling procedures between fluid and solid domains.
- Furthermore, the RKPM shape function is also capable of handling non-uniform fluid grids.

References

1. http://dilbert.engr.ucdavis.edu/~suku/xfem/
2. C. Daux, N. Moës, J. Dolbow, N. Sukumar and T. Belytschko (2000), "Arbitrary Branched and Intersecting Cracks with the Extended Finite Element Method," IJNME, Vol. 48, Number 12, pp. 1741–1760 .
3. N. Sukumar, N. Moës, B. Moran and T. Belytschko (2000), "Extended Finite Element Method for Three-Dimensional Crack Modelling," IJNME, Vol. 48, Number 11, pp. 1549–1570.
4. N. Sukumar, D. L. Chopp, N. Moës and T. Belytschko (2001), "Modeling Holes and Inclusions by Level Sets in the Extended Finite–Element Method," CMAME, Vol. 190, Number 46–47, pp. 6183–6200.
5. L. Zhang, A. Gerstenberger, X. Wang, W.K. Liu, Immersed finite element method, CMAME. 193(21–22) (2004) 2051–2067.
6. W. K. Liu, Y. Liu, D. Farrell, L. Zhang, X. Wang, Y. Fukui, N. Patankar, Y. Zhang, C. L. Bajaj, J. Lee, J. Hong, X. Chen, H. Hsu. Immersed Finite Element Method and Its Applications to Biological Systems. CMAME, 195(13-16):1722-1749, 2006.